25th ABCM International Congress of Mechanical Engineering
October 20-25, 2019, Uberlândia, MG, Brazil

COBEM-2019-1607
EXPERIMENTAL INVESTIGATION OF A STRIP FINS HEAT SINK

William D. P. Fonseca
Rafael F. R. Rosa
School of Mechanical Engineering, University of Campinas, SP - Brazil
fonsecawdp@gmail.com
rafael.franziin@gmail.com
Carlos A. C. Altemani
School of Mechanical Engineering, University of Campinas, SP - Brazil
altemani@fem.unicamp.br

Abstract. *An experimental investigation was performed to obtain the flow and convective heat transfer characteristics of an inline strip fin heat sink cooled by forced airflow. Laboratory tests were conducted under steady state conditions with a heat sink mounted in a rectangular duct with no tip bypass. To present the thermal results, a convective thermal resistance model was adopted and the heat transfer coefficient was based on the flow inlet temperature in the heat sink. The experimental results included the flow pressure drop through the heat sink, the average Nusselt number of the flow in the interfin channels and the heat sink thermal resistance. A comparison was made with results predicted by correlations from the literature for a parallel plates heat sink with the same geometry of the strip fins heat sink. The results indicated that for the same flow rate, the strip fins heat sink presents a larger airflow pressure drop, but its average Nusselt number is larger, so that this heat sink presents a smaller thermal resistance.*

Keywords: *Heat sink, Inline strip fins, Experimental results*

1. INTRODUCTION

The continuous increase of the heat flux from electronic components and devices presents a big challenge to the industry in order to keep their temperature within the manufacturers' specifications for a reliable life cycle (Gurrum *et al.*, 2004). In order to overcome any electronic failures that may emerge from an undesirable temperature increase, a series of innovative cooling techniques have been developed, including the use of phase change materials, thermoelectric cooling, liquid cooling techniques, high conductive fillings and termal interface materials, as presented in Hajmohammadi *et al.* (2013) and Hopton and Summers (2013). In spite of all these efforts, forced convection air cooling still remains the most employed mechanism for the general cooling of electronic equipment. It is mainly so when the temperature control must be attained with minimum cost. In this case, atmospheric air is the cooling fluid, due to its availability, handling facility and dielectric properties.

Due to its thermal properties (relatively small specific mass and thermal conductivity), the forced convection air cooling is usually employed with finned heat sinks, in order to prevent higher temperatures. The fins increase the convective heat transfer area and they may increase the heat transfer coefficient, as well as the conductive and radiative heat losses from the electronic components. Among the heat sinks, that with straight fins of constant cross section is the simplest and the most widely encountered (Churchill and Usagi, 1972; Teertstra *et al.*, 2000; Jonsson and Moshfegh, 2001; Shaeri and Yaghoubi, 2009). It is usually employed with a parallel forced airflow in the interfin channels and the base plate. From the flow entrance in these channels, there is a development of the velocity and thermal boundary layers, which increase the heat sink convective thermal resistance along the flow. This increase may be reduced by a partition of the continuous fins into strip fins of smaller length. The strip fins heat exchange area is reduced in comparison to the heat sink of the same size with continuous straight fins. This area reduction may however be compensated by an increase of the average heat transfer coefficient of the strip fins.

This eventual heat transfer enhancement has led to several studies presented in the literature. Sparrow *et al.* (1977) presented a numerical investigation of the laminar flow and heat transfer from channels with periodical strip fins along the flow direction. The numerical results were obtained for a range of Reynolds numbers and for several values of a dimensionless geometrical parameter. They indicated that the partition of a single longitudinal fin into smaller strip fins reduces the boundary layers growth and thus the strip fins convective thermal resistance.

Sparrow and Liu (1979) compared numerical results for the convective heat transfer and the pressure drop for the laminar flow along continuous fins and strip fins with inline and staggered arrangements. Their results showed that for constant mass flow rate and heat transfer area, the strip fins thermal efficiency is considerably larger than that of the continuous fins. Their results also indicated that the staggered strip fins arrangement presented a better thermal performance than the inline arrangement. A numerical analysis of the comparative performance of the inline and staggered geometrical distribution of strip fins was performed by Al-Sallami *et al.* (2016). Their investigation included the effects of perforated fins to enhance the convective heat transfer. Their results also indicated that the staggered fins arrangement gives a larger heat transfer rate, at the expense of a larger flow pressure drop. Ozturk and Tari (2008) performed a numerical investigation of heat sinks with strip fins applied to the CPU of a computer. They investigated the effects of the number of fins and their distribution, as well as the fins material and the heat sink base thickness.

Other investigations were also performed with the purpose to optimize the geometrical parameters of the strip fins heat sinks. Teertstra *et al.* (1999) developed an analytical model to predict the heat transfer rate from heat sinks with inline strip fins. They indicated that for a range of Reynolds numbers ($40 < Re < 180$), the best configuration for the inline strip fins is that with a ratio of fins spacing (S) to pitch (P) equal to $(S/P) = 0.5$ and for a ratio of fins pitch to baseplate length in the range $0.059 < P/L < 0.44$. Hong and Cheng (2009) also presented numerical results to optimize the geometrical parameters of strip fins heat sinks. They indicated that there is an optimal strip length to minimize the flow pressure drop and that it is independent of both the heat transfer distribution on the heat sink base and its maximum temperature.

The purpose of this work is to present the results of an experimental investigation to obtain the thermal and flow characteristics of a strip fin heat sink cooled by forced airflow in the laboratory. Thus, the experimental results for the airflow pressure drop through the strip fins heat sink, the average Nusselt number in the interfin channels and the convective thermal resistance will be presented. These results will be compared with results obtained with correlations from the literature for a similar parallel plates heat sink.

2. EXPERIMENTAL INVESTIGATION

2.1 Assembly and test procedure

An aluminum strip fin heat sink, as indicated in Fig. 1, with the dimensions presented in Tab. 1, was tested in the laboratory. The heating was obtained by electric power dissipation in a plate resistance (16 Ω) mounted with good thermal contact on the heat sink base. This resistance was made from the winding of a Teflon coated Chromel wire (d = 0,254 mm) on a rectangular phenolic plate machined on one side with thirteen 0.5 mm square grooves. The rectangular plate was 1.2 mm thick and its face had almost the same dimensions of the heat sink base, as indicated in Tab. 1. The plate side with the resistance wire was attached to the heat sink base with a commercial thermal paste (Implastec). To perform the tests, the heat sink was inserted in a rectangular duct made of Plexiglas (k = 0.20 W/m.K), so that the fins base was flush mounted to a channel wall and the fins tips touched the duct opposite wall, so that there was no top bypass. On the sides of the two heat sink lateral fins, the spacing to the duct walls was equal to one half of the interfin channels. The heat sink was located 1 cm downstream of the duct entrance with rounded corners to provide a uniform velocity just upstream the heat sink. After assembling the heat sink with the resistance plate in the duct, it was insulated by a 25 mm layer of polystyrene (k = 0.033 W/m.K). Forced airflow to the duct was provided in suction mode by a downstream fan. For this purpose, the duct was connected to a plenum box with a partition wall where the forced airflow was measured by a calibrated nozzle, as indicated in Fig. 2. Downstream of the plenum box, a tube with a control valve was connected to the suction fan located outside the laboratory.

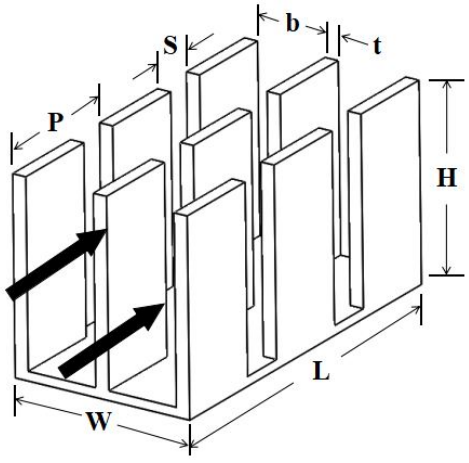

Figure 1. Illustration of an inline strip fins heat sink

Table 1. Geometric parameters of the heat sink and heater

Heat sink		**Heater**	
Parameter	Values	Parameter	Values
L	90 mm	L	85 mm
W	41.5 mm	W	42 mm
t	0.86 mm	t	1.2 mm
b	1,85 mm		
H	14,6 mm		
S	5 mm		
P	14 mm		

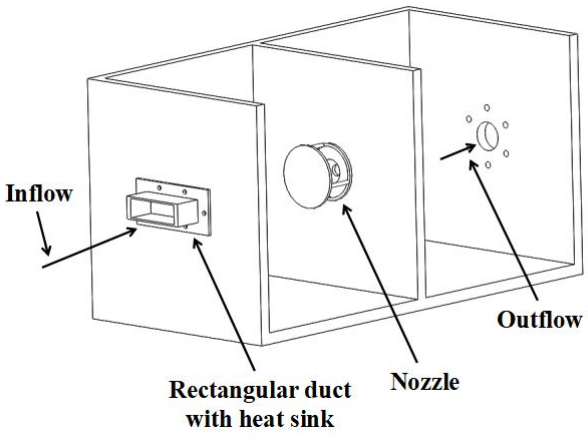

Figure 2. Illustration of a experimental apparatus

The airflow pressure drop through the heat sink was measured under steady, isothermal ambient conditions. The airflow rate in the duct was varied by means of a control valve in the downstream tube the plenum box and it was measured by the previously calibrated flow nozzle in the plenum box. An inclined manometer was used to measure the flow pressure drop through the nozzle. The airflow pressure drop through the heat sink for any flow rate was measured by a calibrated differential pressure transducer (PX750-06DI, Omega Eng.). This transducer was calibrated just before these measurements and its output was an electric current proportional to the measured pressure difference. In these tests, the measured the pressure drop was that from the ambient air in the laboratory to a pressure tap in the rectangular duct, located 30 mm downstream of the heat sink. Two pressure drop tests were performed: one with the heat sink in the duct and the other for the duct without the heat sink. The results to be presented for the airflow pressure drop through the heat sink were obtained subtracting the later measurement from the former. Thus, the resulting pressure drop is due only to the effect of the heat sink on the airflow pressure drop.

The thermal tests were performed with the heat sink base temperature around 40°C. The electric power dissipation in the heating resistance was provided by a dc power supply (Instrutherm FA-3005) and it was evaluated by measuring the electric current and the heating resistance voltage drop by a digital multimeter (34401A, HP). The heat sink and duct were instrumented with eight thermocouples measured with a digital temperature indicator (DP41-TC, Omega Eng.), with a resolution of 0.1°C. The heat sink base had three thermocouples located 2 mm below the fins base and distributed along one diagonal line. The other five thermocouples were located at the duct entrance (1), on the heater (1), on the duct (2) and on the insulation layer (1). Thirteen experimental tests were performed, encompassing a range of the airflow average velocities in the interfin channels from 4 m/s to 20 m/s. The measurements of each test were obtained under steady state conditions, assumed when all the temperature readings were within 0.1°C during a time interval of 30 minutes.

2.2 Data reduction

During the tests, the airflow rate was obtained from the flow pressure drop through the nozzle in the plenum box. It was measured by an inclined manometer filled with pure ethanol (relative specific mass 0.7876) as:

$$\Delta P_{12} = \rho g \Delta h_{12} \tag{1}$$

In Eq. (1), ρ represents the manometric fluid specific mass, Δh_{12} indicates the height of the liquid in the manometer, and g is the gravity constant. This pressure drop was used to obtain the mass flow rate from the nozzle equation:

$$\dot{m}_b = k_b A_t \sqrt{2\rho_a \Delta P_{12}} \tag{2}$$

The air density ρ_a was obtained from the ideal gas law and the nozzle flow coefficient k_b was obtained from a previous calibration in the laboratory as:

$$k_b = \frac{1,111}{Re_b^{0,015}} \tag{3}$$

The airflow Reynolds number through the nozzle was related to its mass flow rate in the form:

$$Re_b = \frac{4\dot{m}_b}{\mu \pi D_b} \tag{4}$$

The air viscosity was expressed as a function of the temperature, as in Sutherland's equation (Incropera *et al.*, 2007). Combining equations (1) to (4), the nozzle Reynolds number was expressed in closed form as:

$$Re_b = \left(\frac{4.1,111.A_b.\sqrt{2\rho_a \Delta P_{12}}}{\mu \pi D_b} \right)^{\frac{1}{1,015}} \tag{5}$$

Once the nozzle Reynolds number is evaluated from this equation, Eq. (4) gives the nozzle mass flow rate, which is the same as that through the rectangular duct with the heat sink. The average airflow velocity (V_{av}) in all the 17 heat sink interfin channels was obtained from this mass flow rate. This average velocity was employed to define an interfin channel Reynolds number based on each interfin channel hydraulic diameter D_h:

$$Re_c = \frac{V_{av} D_h}{\nu} \tag{6}$$

The thermal tests were performed under steady state conditions with the heat sink base temperature around 40°C. The heat sink forced convection to the airflow (q_{cv}) was evaluated by an energy balance under steady state conditions. For this, several thermal losses (q_l) were estimated and subtracted from the electric power dissipation (P_d) in the resistance heater at the heat sink base. These losses included thermal radiation from the heat sink base and fins, conduction through the thermal insulation around the heat sink, and conduction through the power and thermocouple wires. In all the tests, the total thermal losses were limited to 3% of the total power dissipation in the heat sink heater. This balance is expressed by Eq. (7).

$$q_{cv} = P_d - \Sigma q_l \tag{7}$$

This convective heat transfer rate was employed in the convective thermal resistance model, as described by Incropera *et al.* (2007).

$$q_{cv} = h^* [A_c + A_f \eta_f] (\overline{T}_b - T_\infty) \tag{8}$$

In this equation, h^* is the average heat transfer coefficient of the heat sink in contact with the airflow, based on the inlet flow temperature. The fins efficiency is represented by η_f and the fins tips were assumed adiabatic, due to the reported experimental assembly. The tested heat sink had 80 strip fins (16 rows, each with five strip fins) with the dimensions presented in Tab. 1. The total fins heat transfer area is A_f and each fin has a cross sectional area S_c and a perimeter P. The heat sink base area not covered by the fins is A_c.

$$\eta_f = \frac{\tanh(mH)}{mH} \tag{9}$$

$$m = \sqrt{\frac{\overline{h} P}{k_f A_s}} \tag{10}$$

The purpose of Eq. (8) is to obtain an experimental value for the average convective heat transfer coefficient h^*, based on the flow inlet temperature in the duct. The solution was obtained iteratively (MATLAB), since the fin efficiency depends on the average heat transfer coefficient. The evaluated heat transfer coefficient was used to define an average Nusselt number as:

$$Nu = \frac{h^* D_h}{k_{ar}} \tag{11}$$

The experimental results were also used to obtain the heat sink thermal resistance by:

$$R_{th} = \frac{(\overline{T}_b - T_\infty)}{q_{cv}} \tag{12}$$

2.3 Uncertainty analysis

A spreadsheet was developed in the EES (Engineering Equation Solver - F-Chart Software) program for the uncertainties analysis of the experimental results based on the method of uncertainties propagation (Coleman and Steele, 2018). Considering a result S, obtained by n experimental measurements x_i, the uncertainty of S (denominated σ_S) can be calculated by:

$$\sigma_S = \sqrt{\sum_{i=1}^{N} \left(\frac{\partial S}{\partial x_i} \Delta x_i \right)^2} \tag{13}$$

The absolute or relative uncertainties of all measurements were specified, along with the nominal measurements of each test. The results and their uncertainties were then obtained for each experimental test performed. The absolute uncertainties for the readings of the inclined manometer, U-manometer and thermocouples were estimated according to Tab. 2. For the aluminum and air properties, relative uncertainties of 1% of the tabulated values were assumed. These uncertainties were inserted in the EES worksheet to obtain the uncertainty values for the mass air flow rate, the Reynolds number, the convective heat transfer rate and the airflow pressure drop.

Table 2. Values adopted for uncertainties.

Variable	Uncertainties
Inclined manometer hight [in alcohol]	0.005
U-Manometer height [mmca]	0.5
Thermocouple temperature [°C]	0.1
Barometric pressure [hPa]	5.0
Coefficient K of the nozzle [-]	0.02
Aluminum properties [%]	2.5
Air properties [%]	1.0

3. COMPACT MODEL FOR THE PLATE FINS HEAT SINKS

The compact model for the plate fins heat sinks was obtained from Tomazeti and Altemani (2002) comprising correlations for the airflow pressure drop through the heat sink and for the convective heat transfer coefficient in the interfin channels.

3.1 Pressure drop

The pressure drop was obtained for rectangular ducts with aspect ratio $\alpha \leq 1$, based on the duct hydraulic diameter D_h. The friction pressure losses were evaluated with the apparent Fanning friction factor f_a, so that the total head loss through the heat sink was expressed by:

$$\Delta P = 4 f_a \frac{L}{D_h} \rho \frac{V^2}{2} + K_e \rho \frac{V^2}{2} \tag{14}$$

For laminar flow the apparent friction factor f_a was approximated by:

$$f_a Re_c = \frac{3.435}{X^{0.5}} + \frac{16\phi^{-1} + 1.25(4X)^{-1} - 3.435X^{-0.5}}{1 + 0.00021X^{-2}} \tag{15}$$

In Eq. (15), ϕ and X and are expressed as:

$$\phi = \frac{2}{3} + \frac{11}{24}\alpha(2 - \alpha) \tag{16}$$

$$X = \frac{L/D_h}{Re_c} \tag{17}$$

For turbulent flow, the apparent friction factor was obtained from a correlation presented in Phillips (1988) as:

$$f_a = A(\phi . Re_c)^B \tag{18}$$

Where $A = 0.0929 + \frac{1.01612}{L/D_h}$ and $B = -0.26800 - \frac{0.31930}{L/D_h}$.

The expansion coefficient K_e in Eq. (14) is expressed in Eq. (19), where the coefficients A_i and B_i are presented in Tab. 3.

$$K_e = (1-\alpha)(A_0 + A_1\sigma + A_2\sigma^2) + \alpha(B_0 + B_1\sigma + B_2\sigma^2) \tag{19}$$

Table 3. Coefficients for Eq. (19)

	Expansion Coefficient K_e	
	Laminar regime	Turbulent regime
A_0	1	1
A_1	-2.4	-2.083
A_2	1	1.005
B_0	1	1
B_1	-2.8	-2.125
B_2	1	0.976

3.2 Convective heat transfer

The convective heat transfer rate was expressed by:

$$q_{cv} = h^* A_t \eta_0 (\overline{T}_b - T_\infty) \tag{20}$$

In this equation h* was based on the incoming airflow temperature and η_0 is the standard heat sink overall thermal efficiency:

$$\eta_0 = 1 - \frac{A_f}{A_t}(1-\eta_f) \tag{21}$$

A_f and A_t are the finned and total heat transfer areas and the fin efficiency (η_f) was obtained from Eq. (9).

For laminar flows in the interfin channels, the average Nusselt number was obtained from a correlation valid for the entrance region of a parallel plates channel with uniform temperature and velocity profiles at the entrance and isothermal walls, valid for Pr ≈ 1.

$$\overline{Nu}^* = \frac{h^* D_h}{K} = \frac{0.664\sqrt{G_Z}}{Pr^{1/6}}\sqrt{1 + 7.3\sqrt{\frac{Pr}{G_Z}}} \tag{22}$$

Where $G_Z = \frac{RePr}{L/D_h}$.

For turbulent flow, average Nusselt number in the entrance region of the rectangular duct was obtained from:

$$\overline{Nu} = \frac{\overline{h} D_h}{k} = Nu_\infty \left[1 + \frac{2.4254}{(L/D_h)^{0.676}}\right] \tag{23}$$

The value of Nu_∞ was obtained from Gnielinski equation, where the fully developed Fanning friction factor was obtained from the Blasius equation :

$$f = \frac{0.079}{Re_c^{0.25}} \tag{24}$$

$$Nu_\infty = \frac{(f/2)(\phi Re_b - 1000)Pr}{1 + 12.7(f/2)^{0.5}(Pr^{0.67} - 1)} \tag{25}$$

Since $\overline{h}$ in Eq. (23) was based on the fluid mean bulk temperature, the value of h^* was then obtained from:

$$h^* = \frac{\dot{m} c_p}{A_t \eta_0}\left[1 - exp\left(\frac{\overline{h} A_t \eta_0}{\dot{m} c_p}\right)\right] \tag{26}$$

This is a standard conversion to the heat transfer coefficient based on the fluid entrance temperature as reference.

4. RESULTS AND DISCUSSION

The experimental tests were performed with an aluminum strip fins heat sink with the dimensions presented in Tab. 1, comprising 16 parallel rows of strip fins. Each row had five strip fins separated from each other with uniform spacing. The average airflow velocity in the interfin channels varied from 4 to 20 m/s. The corresponding interfin channels Reynolds number based on their hydraulic diameter was in the range from 800 to 3,900. For comparison purposes, results from correlations for a plate fins heat sink presented in Tomazeti and Altemani (2002) were evaluated for a heat sink with the same geometry and they are compared with the experimental results from the strip fins heat sink.

The measured airflow pressure drop in the heat sink is presented in Fig. 3 as a function of the average airflow velocity in the interfin channels. The test data show a monotonic increase of the flow pressure drop with the channels velocity. This behavior is similar to that observed in the literature, for example, in Al-Sallami *et al.* (2016). It is observed that when compared to the curve obtained from the correlation for the plate fins heat sink, Eq. (14), the airflow pressure drop for the strip fins heat sink is increasingly larger, indicating the need of larger pumping power as the airflow velocity increases. At the smallest tested velocity, the pressure drop for both heat sinks is about the same.

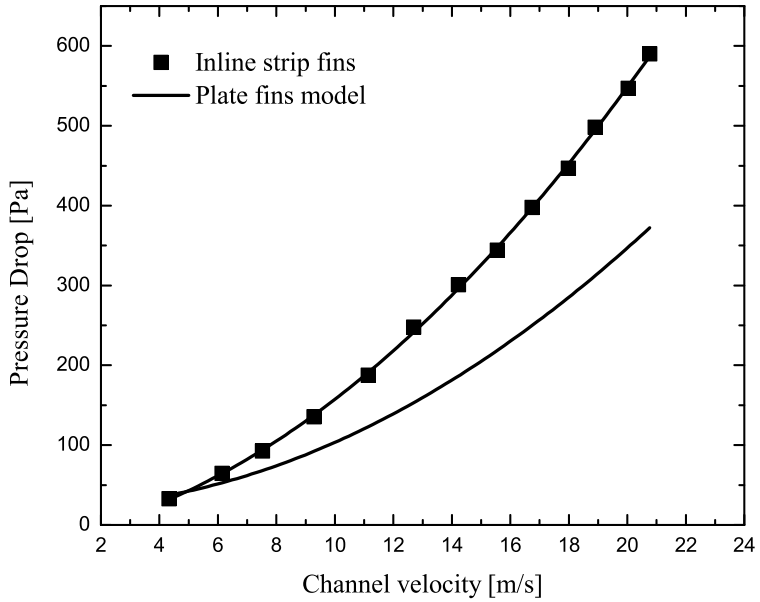

Figure 3. Pressure drop from the experimental data for the strip fins heat sink and from the correlation for the flat plate heat sink

The experimental data for the average heat transfer coefficient (using the flow inlet temperature as reference) were obtained from Eqs. (8), (9) and (10) and they were used to evaluate the average Nusselt number as in Eq. (11). The results are presented in the Fig. 4 as a function of the channel Reynolds number Re_c defined by Eq. (6). The average Nusselt increases with the channel Reynolds number and a single correlation could be used to fit all the experimental data in the form Nu = c ${Re_c}^m$, where c = 0.028 and m = 0.77. This behavior of the average Nusselt number reflects the complex flow and convective heat transfer in the channels with the inline strip fins. The strip fins in these channels induce the flow to separate at the downstream end of each fin and to start new boundary layers at the downstream strip fin, and so on. They must induce turbulent flow at low channel Reynolds number as indicated by the single correlation encompassing all the data. On the other hand, the results from the correlations for the similar heat sink with plate fins were expressed in distinct form for the laminar and for the turbulent flow regimes. They are also presented in Fig. 4, showing that as the Reynolds number increases, the strip fins present a pronounced increase of the average Nusselt number.

The data for the heat sink convective thermal resistance are presented in Fig. 5 and they show a typical decrease with the average airflow velocity in the interfin channels. This result reflects the increase of the convective heat transfer from the heat sink with the airflow rate in the interfin channels, as was indicated in Fig. 4. The correlations data for the plate fins heat sink were also used to obtain its thermal resistance, as indicated in Fig. 5. They show a similar decrease with the average airflow velocity in the fins channels, but the strip fins heat sink data presented smaller thermal resistance. These results show that in spite of the smaller heat transfer area of the strip fins heat sink, the average heat transfer coefficient is larger enough to give rise to smaller thermal resistance. One should keep in mind however that the strip fins heat sink demands larger pumping power for the same airflow velocity.

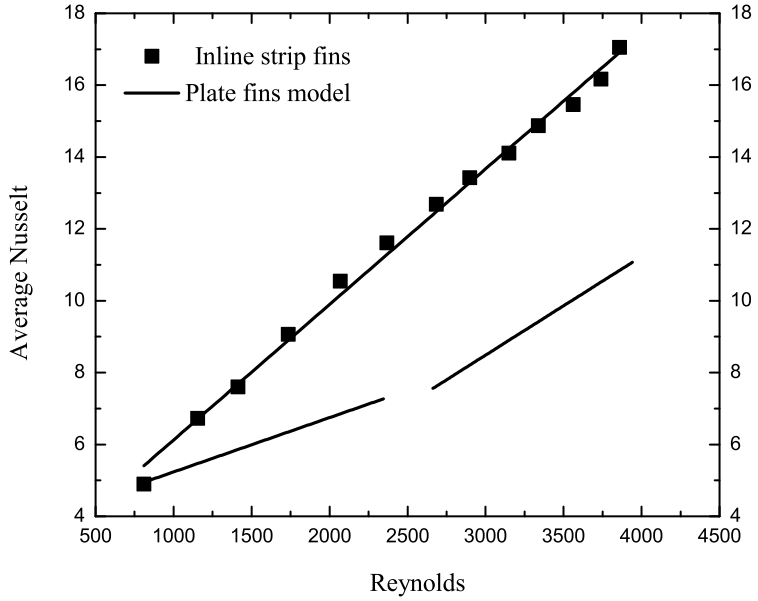

Figure 4. The average Nusselt number from the experimental data for the strip fins heat sink and from the correlation for the flat plate heat sink

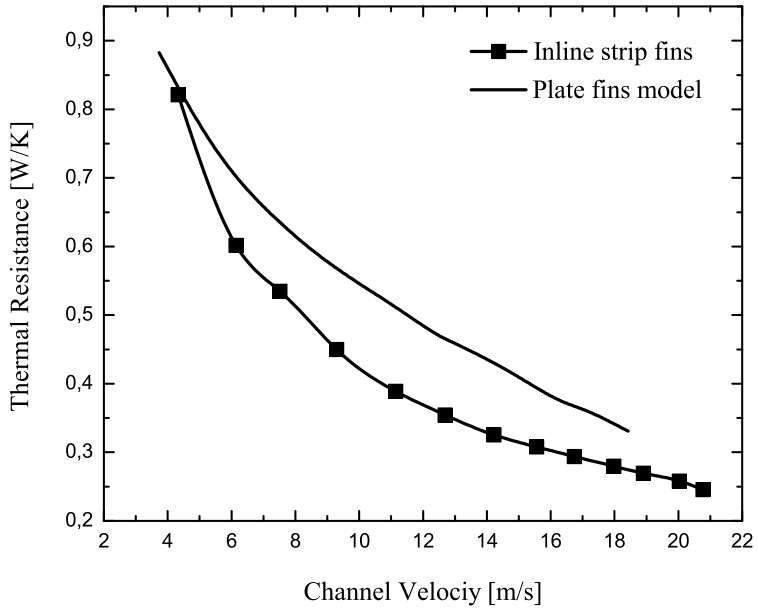

Figure 5. The thermal resistance from the experimental data for the strip fins heat sink and from the correlation for the flat plate heat sink

5. CONCLUSIONS

Experimental tests were performed with an inline strip fins heat sink to obtain the airflow pressure drop through the heat sink, the average heat transfer coefficient based on the inlet flow temperature and the heat sink thermal resistance. These results were compared to similar results obtained for a parallel plates heat sink with the same geometry, based on correlations from the literature. The strip fins heat sink require a larger pumping power for any airflow rate, but they have smaller thermal resistance. In spite of the smaller heat transfer area, the strip fins presented larger heat transfer coefficients with the forced airflow, enough to give rise to smaller thermal resistance.

6. ACKNOWLEDGEMENTS

The support of FAPEMA, the Foundation of Research and Scientific Development of Maranhão, in the form of a Scholarship to the first author, is deeply appreciated.

7. REFERENCES

Al-Sallami, W., Al-Damook, A. and Thompson, H., 2016. "A numerical investigation of thermal airflows over strip fin heat sinks". *International Communications in Heat and Mass Transfer*, Vol. 75, pp. 183–191.

Churchill, S. and Usagi, R., 1972. "A general expression for the correlation of rates of transfer and other phenomena". *AIChE Journal*, Vol. 18, No. 6, pp. 1121–1128.

Coleman, H.W. and Steele, W.G., 2018. *Experimentation, validation, and uncertainty analysis for engineers*. John Wiley & Sons.

Gurrum, S.P., Suman, S.K., Joshi, Y.K. and Fedorov, A.G., 2004. "Thermal issues in next-generation integrated circuits". *IEEE Transactions on device and materials reliability*, Vol. 4, No. 4, pp. 709–714.

Hajmohammadi, M., Abianeh, V.A., Moezzinajafabadi, M. and Daneshi, M., 2013. "Fork-shaped highly conductive pathways for maximum cooling in a heat generating piece". *Applied Thermal Engineering*, Vol. 61, No. 2, pp. 228–235.

Hong, F. and Cheng, P., 2009. "Three dimensional numerical analyses and optimization of offset strip-fin microchannel heat sinks". *International Communications in Heat and Mass Transfer*, Vol. 36, No. 7, pp. 651–656.

Hopton, P. and Summers, J., 2013. "Enclosed liquid natural convection as a means of transferring heat from microelectronics to cold plates". In *29th IEEE Semiconductor Thermal Measurement and Management Symposium*. IEEE, pp. 60–64.

Incropera, F.P., Lavine, A.S., Bergman, T.L. and DeWitt, D.P., 2007. *Fundamentals of heat and mass transfer*. Wiley.

Jonsson, H. and Moshfegh, B., 2001. "Modeling of the thermal and hydraulic performance of plate fin, strip fin, and pin fin heat sinks-influence of flow bypass". *IEEE Transactions on Components and Packaging Technologies*, Vol. 24, No. 2, pp. 142–149.

Ozturk, E. and Tari, I., 2008. "Forced air cooling of cpus with heat sinks: A numerical study". *IEEE transactions on components and packaging technologies*, Vol. 31, No. 3, pp. 650–660.

Phillips, R.J., 1988. "Microchannel heat sinks". *The Lincoln Laboratory Journal*, Vol. 1, No. 1, pp. 31–48.

Shaeri, M. and Yaghoubi, M., 2009. "Thermal enhancement from heat sinks by using perforated fins". *Energy conversion and Management*, Vol. 50, No. 5, pp. 1264–1270.

Sparrow, E., Baliga, B. and Patankar, S., 1977. "Heat transfer and fluid flow analysis of interrupted-wall channels, with application to heat exchangers". *Journal of Heat Transfer*, Vol. 99, No. 1, pp. 4–11.

Sparrow, E. and Liu, C., 1979. "Heat-transfer, pressure-drop and performance relationships for in-line, staggered, and continuous plate heat exchangers". *International Journal of Heat and Mass Transfer*, Vol. 22, No. 12, pp. 1613–1625.

Teertstra, P., Culham, J. and Yovanovich, M., 1999. "Analytical modeling of forced convection in slotted plate fin heat sinks". *ASME-PUBLICATIONS-HTD*, Vol. 364, pp. 3–12.

Teertstra, P., Yovanovich, M. and Culham, J., 2000. "Analytical forced convection modeling of plate fin heat sinks". *Journal of Electronics Manufacturing*, Vol. 10, No. 04, pp. 253–261.

Tomazeti, C.A. and Altemani, C.A., 2002. "A compact model for heat sinks with experimental verification". *8th THERMINIC Workshop*, Vol. 1, p. 530.

8. RESPONSIBILITY NOTICE

The authors are the only responsible for the printed material included in this paper.